SCIENCE CHINA
Physics, Mechanics & Astronomy

• Research Paper •
Special Issue: Forward for the Department of Engineering Mechanics, Tsinghua University

April 2011 Vol.54 No.4: 783–791
doi: 10.1007/s11433-011-4290-4

Dynamic modelling and analysis of space webs

YU Yang*, BAOYIN HeXi & LI JunFeng

School of Aerospace, Tsinghua University, Beijing 100084, China

Received December 12, 2010; accepted February 15, 2011; published online February 28, 2011

Future space missions demand operations on large flexible structures, for example, space webs, the lightweight cable nets deployable in space, which can serve as platforms for very large structures or be used to capture orbital objects. The interest in research on space webs is likely to increase in the future with the development of promising applications such as Furoshiki sat-ellite of JAXA, Robotic Geostationary Orbit Restorer (ROGER) of ESA and Grapple, Retrieve And Secure Payload (GRASP) of NASA. Unlike high-tensioned nets in civil engineering, space webs may be low-tensioned or tensionless, and extremely flexible, owing to the microgravity in the orbit and the lack of support components, which may cause computational difficulties. Mathematical models are necessary in the analysis of space webs, especially in the conceptual design and evaluation for prototypes. A full three-dimensional finite element (FE) model was developed in this work. Trivial truss elements were adopted to reduce the computational complexity. Considering cable is a compression-free material and its tensile stiffness is also variable, we introduced the cable material constitutive relationship to work out an accurate and feasible model for prototype analysis and design. In the static analysis, the stress distribution and global deformation of the webs were discussed to get access to the knowledge of strength of webs with different types of meshes. In the dynamic analysis, special attention was paid to the impact problem. The max stress and global deformation were investigated. The simulation results indicate the interesting phenomenon which may be worth further research.

space webs, finite element method, cable material, nonlinear constitutive relationship

PACS: 98.70.Sa, 90.50.sb, 13.85.Tp

1 Introduction

Future space missions demand operations on large flexible structures such as solar sails, large solar panels and reflector antennas. Several recent studies [1–7][1–3] indicate an interest increasing in space webs, which can serve as platforms for large structures or be used to capture orbital objects.

An idea of cable webs applied in space missions was put forward by Nakasuka et al. [1] and Kaya et al. [2,3] for the concept of Furoshiki satellite, in which a deployment scheme [2] for large membrane or mesh structure was developed for phased array antenna constructing. Later, the Japanese space agency JAXA [3] conducted a sounding rocket experiment intended to test several key technologies including the deployment and stabilization of cable webs in a microgravity environment. Meanwhile, the ESA Advanced Concepts Team started a project to investigate the deployment control of space webs from a spinning satellite [6,7].

Another widely concerned application of space webs is to capture orbital objects, one intention of which is to reduce the population of large orbital debris. Tethers Unlimited Inc (TUI)[1,2], in collaboration with NASA, developed a technology called "Grapple, Retrieve And Secure Payload" (GRASP)[1], which will enable small spacecrafts to capture space debris objects, including default spacecraft and upper stages already in orbit. The GRASP uses inflatable booms

*Corresponding author (email: ocean361@163.com)
1) www.wpi.edu/Pubs/E-project/Available/E.../Space_Tethers_IQP.pdf
2) www.tethers.com/papers/DeorbitTechnologies.pdf
3) http://www.esa.int/TEC/Robotics/SEMTWLKKKSE_0.html

to deploy large web structures, which can be maneuvered around a space debris object and then collapsed to securely capture it. Then TUI took tests of GRASP prototype on Zero-G Corp. aircraft, in order to demonstrate the capture of a tumbling object in a microgravity environment[2]. The European Space Agency (ESA) proposed "Robotic Geostationary Orbit Restorer" (ROGER)[3] concept to study on the need for and feasibility of a mission to control the threat from large orbital debris in the geostationary orbit, in which a robotic spacecraft was designed by the ASTRIUM team to capture target objects using 20 throw-nets.

Using cable webs to capture orbital objects is appealing for many reasons.

(1) Since the cable webs are flexible and lightweight, they can be packed into very small volume and be convenient for transportation.

(2) In orbit, cable webs can deploy from the small packages to very big sizes as the mission requires, with good performance of energy consumption.

(3) Cable webs are good buffering devices due to the slackness after deployment, which avoids hard collision and provides reaction time.

(4) Large web section provides sufficient error tolerance, which can efficiently reduce control requirements. As is known, precise control requires expensive equipment and involves high mission risks.

There are also some disadvantages:

(1) The motion of slack webs in a microgravity environment is hard to predict. The risk of entanglement should be decreased by choosing a proper folding pattern and a deployment method.

(2) Cable webs may not be strong enough to resist high velocity impact of orbital debris. Accurate assessment of strength is always necessary.

Mathematical models [8–11] are essential in the analysis of space webs, especially in the conceptual design and evaluation for prototypes. Multiparticle models with spring-mass networks are usually considered, with constants determined experimentally [8]. That means many experiments are required to determine such a large set of constants for an arbitrary model, which is very hard to achieve. The present authors have previously presented a modeling method for project deployment of space webs, in which a flexible multi-body model was developed using Absolute Nodal Coordinate Formulation (ANCF) [12–16]. The project deployment of square web with 100 meshes was computed under different conditions on PC. Then the results found the computing time would become unacceptably long when the number of meshes increased to 400 [12]. Mattias Gärdsback et al. [6] developed a finite element model, implemented in the commercial software LS-DYNA, in order to verify a robust control method for space webs spinning deployment. Fumio Fujii et al. [17,18] introduced a compression-free material law for cable elements in the study of dynamical behavior of flexible and incompressible goal nets for soccer.

In dynamical analysis, the capture process is highly nonlinear due to large deformation, complex structure, incompressible material property and rapidly changing external load. In particular, when unfolded, space webs may be low-tensioned and extremely flexible, owing to the microgravity in orbit and the lack of support components. Space webs are too slack and flexible to resist any compressive force, and thus there may be no formed configurations for them. While in the impact process, there is a sharp increase for internal force in the web and a large deformation during a short time. All the above factors might cause computing problems.

The study aims to develop a numerical method with favorable generality for space webs and to investigate the behavior of cable webs with different meshes in statics and dynamics. A parameterized pre-processing program was developed to generate information of different types of webs including node position and element connectivity. In order to simulate the material nonlinear property of cable, a new material constitutive relationship was introduced into the web's finite element model. Explicit time integration was employed to calculate the static and dynamic response of triangle-mesh, square-mesh and hexagon-mesh webs under different conditions, and the mechanical characteristics of webs with the three meshes in the impact process were obtained.

2 Numerical method

Considering the topology of webs is certain, only the cable segments between nodes deform as the web moves. Supposing the relationship between the elongation and the internal force of a segment can be described accurately, the specific shape of the segment can be ignored without causing too much difference. In this paper, a three-dimensional finite element model of space webs was divided as an assembly of truss elements, and the incompressible property and variable tensile stiffness of cable material were considered and implemented by an inline function containing the cable material property information.

The pre-processing of webs with different types of meshes was implemented, in which the information of node position and element connectivity was calculated and imported. Explicit time integration was employed to solve the governing equations of motion.

2.1 Governing equations

The governing equations of motion can be written as eq. (1). In order to simulate the dynamic behavior of flexible webs, the equations will be integrated:

$$\boldsymbol{M}\ddot{\boldsymbol{u}} + \boldsymbol{C}\dot{\boldsymbol{u}} + \boldsymbol{E}\left(\boldsymbol{u}\right) = \boldsymbol{Q}\left(\boldsymbol{u}, t\right) \tag{1}$$

with mass matrix $\boldsymbol{M}$, acceleration vector $\ddot{\boldsymbol{u}}$, damping matrix $\boldsymbol{C}$, velocity vector $\dot{\boldsymbol{u}}$, external load vector $\boldsymbol{Q}(\boldsymbol{u},t)$ and internal force vector $\boldsymbol{E}(\boldsymbol{u})$.

2.2 Cable material constitutive relationship

To our knowledge, the static and dynamic response of flexible webs are geometrically highly nonlinear, including large nodal displacements and element deformations. And the problem scale increases rapidly with the size of webs. Truss element, with the size equal to the mesh, was adopted in the FE model in order to reduce the computational complexity. However, this discrete method assumes that the cables can be bent only at the nodes, which might cause a great error in simulating the motion of loose webs, so the cable material constitutive relationship was introduced into the model. In some sense, that is to describe the relationship between the elongation and the internal force accurately and ignore the specific shape of the segment.

Cable material constitutive relationship can be described as the incompressible property and variable tensile stiffness, as illustrated in Figure 1. Intuitively, a cable is woven out of fibres, thin and slack in natural state, and the cable's stiffness is the summation of all the fibre's. Stretching from natural length, the web segment has tiny stiffness on both sides, for most fibres are slack. When the web segment is compressed, there is hardly resistance for a sagging segment. However, on the tension side, the state of each fibre in the cable is not synchronized. The cable stiffness increases with the number of tensioned fibres, which leads to a rapid increase of the segment internal force. Beyond this margin of initial slackness, the relationship between the internal force and the elongation becomes linear and elastic, since all fibres become tensioned to resist the stretching force.

Based on the above discussion, here define the relationship between the element internal force and the elongation:

$$T=\frac{1}{2}\left[\left(\Delta-\Delta_0\right)+\sqrt{\left(\Delta-\Delta_0\right)^2+4N^2}\right]\frac{EA}{L}-\alpha EA, \qquad (2)$$

with element axial internal force T, axial elongation Δ, element slackness margin Δ_0, asymptotic factor N, asymptotic stiffness E, element cross section area A, element natural length L, and $\alpha=\left(-\varepsilon_0+\sqrt{\varepsilon_0^2+4\eta^2}\right)\Big/2$.

Define axial stress $\sigma=T/A$, axial strain $\varepsilon=\Delta/L$, reduced slackness margin $\varepsilon_0=\Delta_0/L$, reduced asymptotic factor $\eta=N/L$, and then $\alpha=\left(-\varepsilon_0+\sqrt{\varepsilon_0^2+4\eta^2}\right)\Big/2$, eq. (3) is obtained from eq. (2) (see in Figure 2):

$$\sigma=\frac{1}{2}\left[\left(\varepsilon-\varepsilon_0\right)+\sqrt{\left(\varepsilon-\varepsilon_0\right)^2+4\eta^2}\right]E-\alpha E. \qquad (3)$$

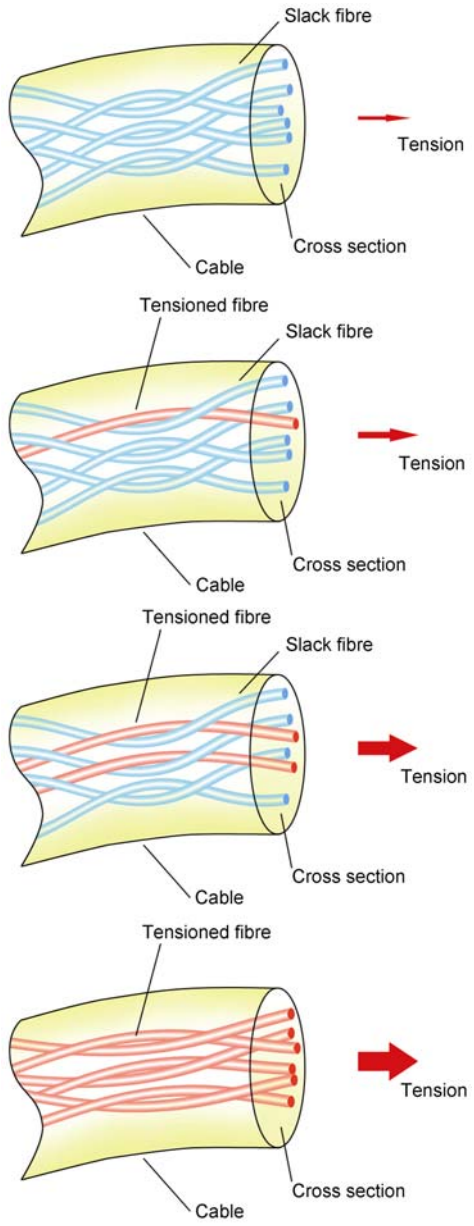

Figure 1 The internal changes in a cable. More fibres turn tight from the slack state as the tension increases until all fibres exceed the margin of initial slackness.

The cable material constitutive relationship was implemented in the FE model by an inline function containing the cable material property information.

2.3 Numeric verification

Numerical examples were employed to test the performance of the above method for the simulation of dynamic behaviours of slack cable and webs.

Example 1 As ref. [6,7] analyzed, the energy variation caused by shearing and bending deformation is the same order of magnitude with the friction and environmental ef-

fects, which is tiny and negligible compared with the tensile force.

In Figure 3, the multiparticle model was introduced to the numeric verification, in which the cable was discreted as mass particles were connected by the extension spring and the torsion spring.

Figure 4 illustrated the shapes of catenary separately calculated with the FE model and the multiparticle model. Suppose a 4.0 meter length cable, with 100 elements or 101 mass particles, cross section area 1.0×10^{-4} m^2 and density 500 kg/m^3. The asymptotic stiffness E is 7×10^7 Pa, which also determines the stiffness of the extension spring and the torsion spring.

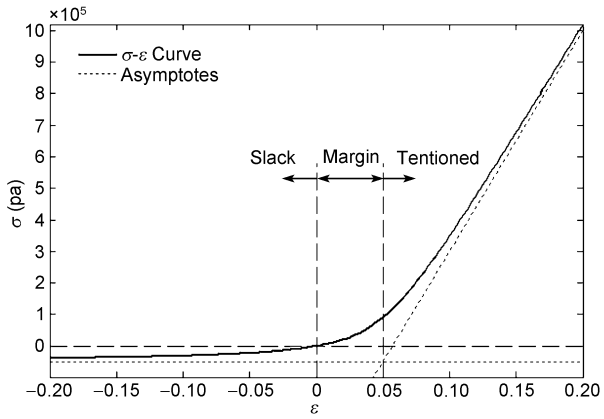

Figure 2 The σ–ε curve, the shape of which is controlled by three parameters ε_0, η and E. According to the definition, initial slackness margin is controlled by ε_0, the smoothness of curve is controlled by η and the slope of asymptotes is controlled by E.

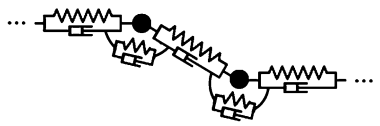

Figure 3 The multiparticle model, in which the tensile force and bending moment were approximated with the extension spring and the torsion spring.

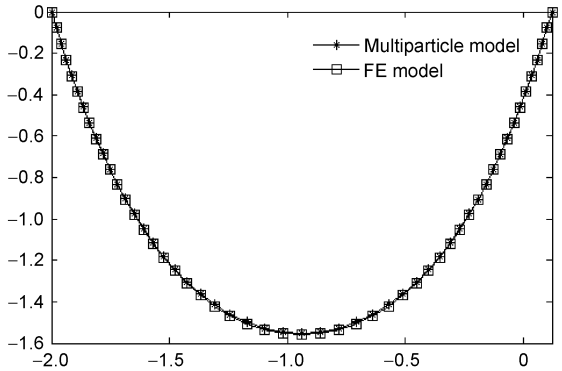

Figure 4 The shapes of catenary with the FE model and the multiparticle model employed. Because of the results, the bending moment was so small that the effects on the deformation could be ignored without causing too many errors.

Example 2 Since the cable is made up of fibres, the dependence of extending, shearing force and bending moment on the deformation is highly nonlinear and probably time-related, which leads to the phenomenon called indifferent balance of long slack cable, i.e. there is no unique equilibrium shape in the microgravity environment.

As Figure 5 illustrated, initially the planar cable is slack in the microgravity environment, and its boundaries are fixed. The cable's total length is 2.0 meters, with 100 elements or 101 mass particles, cross section area 1.0×10^{-4} m^2 and density 200 kg/m^3. The stiffness parameters are the same as those in Example 1. The impact response was separately simulated with the finite element model and the multiparticle model employed.

Figure 6 illustrated the final equilibrium shapes calculated with these two methods.

Example 3 The triangle-mesh webs span as a flat square, with 1540 meshes, 2014 elements and 755 nodes. Define the length of element 0.1 m, cross section area 1.0×10^{-4} m^2, density 200 kg/m^3. Load some concentrated pres-

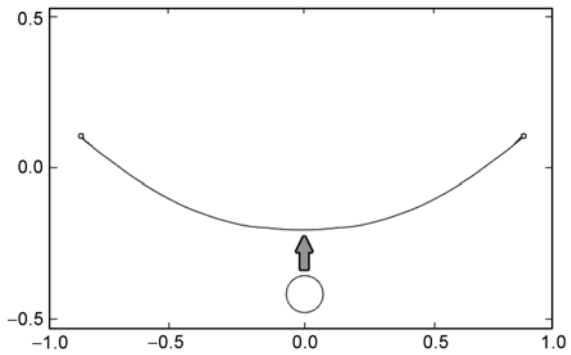

Figure 5 A circle ring with mass 1.0 kg and radius 8 cm impacts the slack cable vertically at a speed of 0.45 m/s. Dynamic responses before and after the impact were simulated with the FE model and the multiparticle model applied.

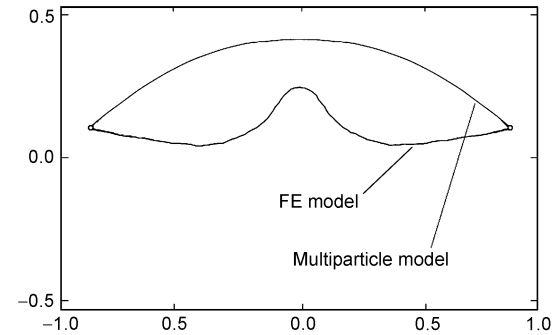

Figure 6 The equilibrium shapes resulting with the two methods applied. Since the truss elements could be bent only at the nodes without producing bending moment, the FE model provided better approximation to the slack cable's feature of indifferent equilibrium.

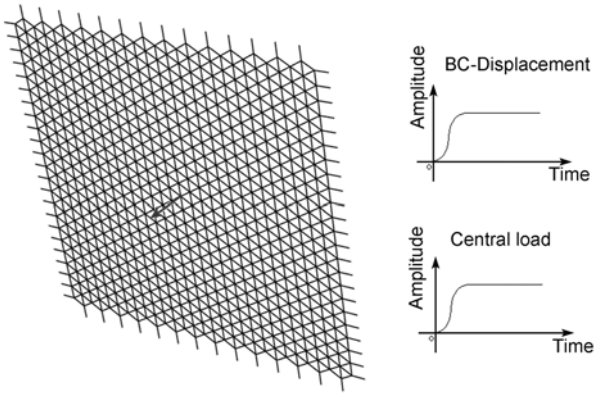

Figure 7 Initial configuration and load and boundary conditions for the verification model.

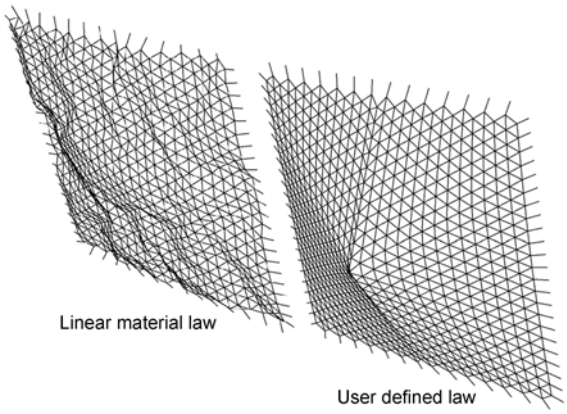

Figure 8 Configurations of triangle-mesh webs in different constitutive laws. In the triangle-mesh webs, some of the elements are compressed and slack, so the linear elastic material leads to an equilibrium state of bar system, while the cable material demonstrates the configuration that the real cable web turns out to be.

sion on the centre of webs, and make the boundary displacement gradual change as Figure 7 shows.

Cable material and linear elastic material were separately introduced into the same web, which leads to different deformations, as illustrated in Figure 8.

3 Analysis of flexible webs

To capture orbital objects is an important application of space webs. In the impact process, slack webs turn to high-tension rapidly, causing a sharp increase of the tension force in the webs. Therefore, cable webs may not be strong enough to resist the high velocity impact of orbital debris. An accurate assessment of strength is always necessary.

In this part of the paper, special attention is paid to the static and dynamic behavior of webs with different meshes: triangle-mesh, square-mesh and hexagon-mesh webs.

3.1 Length-area ration

In order to treat with the ration of cable length and web area h, define the mesh area A, number of layers N, the web area S, and total cable length L.

3.1.1 Triangle-mesh web

As illustrated in Figure 9(a), the number of meshes:

$$(3N-2)^2.$$

The total web area:

$$S=(3N-2)^2 A.$$

The total length of cable;

$$L=\frac{3\sqrt{A}}{\sqrt[4]{3}}(3N-1)(3N-2).$$

According to the above definition, the length-area ration for a large triangle-mesh web is

$$h_{tr}=\lim_{N\to\infty}\frac{L}{S}=\frac{3^{3/4}}{\sqrt{A}}\approx\frac{2.28}{\sqrt{A}}.$$

3.1.2 Square-mesh web

As illustrated in Figure 9(b), the number of meshes:

$$(2N-1)^2.$$

The total web area:

$$S=(2N-1)^2 A.$$

The total length of cable:

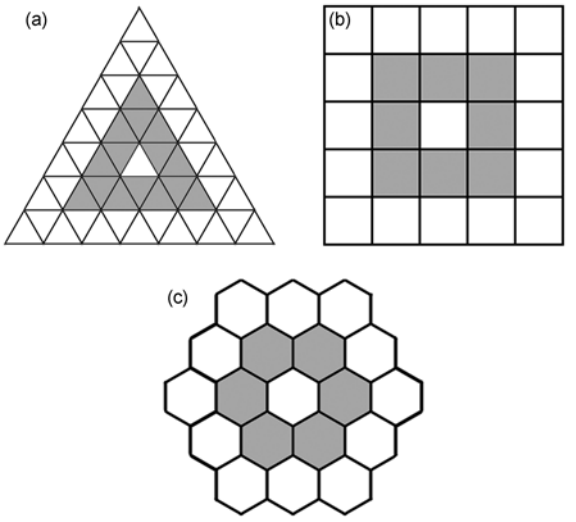

Figure 9 Webs with different meshes, shaded area identified as the layers of different webs, which is marked to calculate the summation of webs' area. (a) Triangle-mesh web; (b) square-mesh web; (c) Hexagon-mesh web.

$$L = 4N(2N-1)\sqrt{A}.$$

According to the above definition, the length-area ration for a large square-mesh web is

$$h_{sq} = \lim_{N\to\infty} \frac{L}{S} = \frac{2}{\sqrt{A}}.$$

3.1.3 Hexagon-mesh web

As illustrated in Figure 9(c), the number of meshes:

$$(2N-1)^2.$$

The total web area:

$$S = (2N-1)^2 A.$$

The total length of cable:

$$L = 4N(2N-1)\sqrt{A}.$$

According to the above definition, the length-area ration for a large hexagon-mesh web is

$$h_{he} = \lim_{N\to\infty} \frac{L}{S} = \frac{3^{1/4}\sqrt{2}}{\sqrt{A}} \approx \frac{1.86}{\sqrt{A}}.$$

As a result, the length-area ration of the hexagon-mesh web is higher than those of the other two, because the hexagon-mesh web is good topology for effectively decreasing the load quality on vehicles.

3.2 Static analysis

Consider the triangle-, square- and hexagon-mesh webs provided with the same length of cable and the same total area. Load the same concentrated pression at the centre point normal to the web on each side; special attention is paid to the stress distribution and the global deformation of webs.

3.2.1 Equilibrium configuration

As illustrated in Figure 10, the equilibrium configurations of three webs differ evidently, since the deformation of the hexagon-mesh web is larger, but concentrated locally.

3.2.2 Stress distribution

To investigate the stress distribution of different webs, we calculate three webs with triangle, square and hexagon meshes under concentrated pression on the centre point.

As Figure 11 illustrated, in the triangle-mesh web, the maximum value of stress appears around the load point, and the stress decreases with the distance from the load point. Some elements are compressed and slack in the web, which contributes nothing to the strength of the whole web. Thus, there is a waste of material in the triangle-mesh web.

As Figure 12 illustrated, in the square-mesh web, the maximum value of stress appears around the load point. The stress concentrates on the two cables that cross at the load point, and the stress on these two cables is almost equally

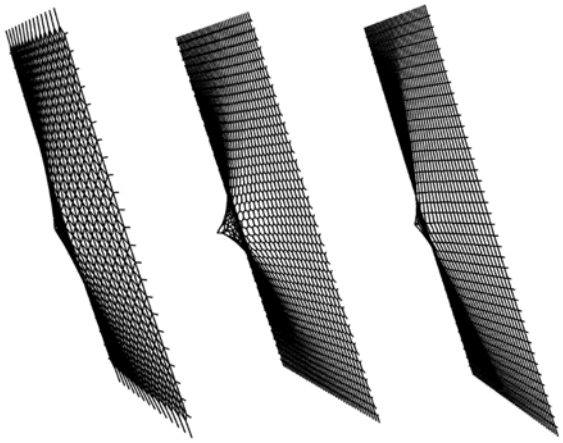

Figure 10 Deformation of webs with different meshes. The vertical displacement of the load point is obviously different.

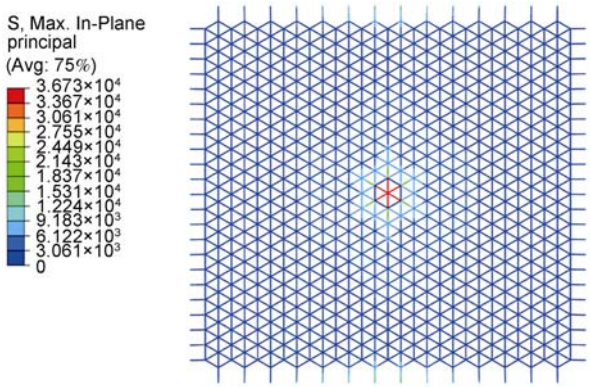

Figure 11 Stress distribution of a triangle-mesh web, with the number of meshes 1260, the number of elements 2014, and the number of nodes 755. The web's initial state is flat and slack, and the boundaries are fixed tightly.

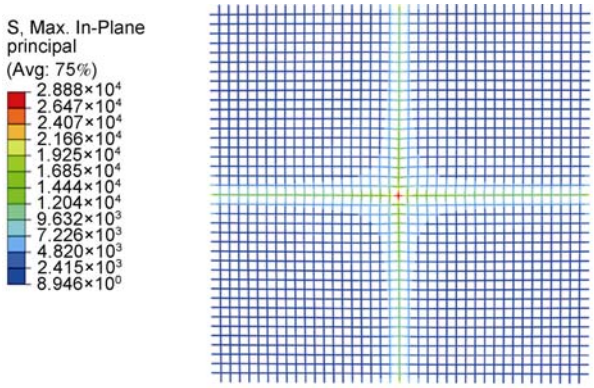

Figure 12 Stress distribution of a square-mesh web, with the number of meshes 1600, the number of elements 3120, and the number of nodes 1677. The web's initial state is flat and slack, and the boundaries are fixed tightly.

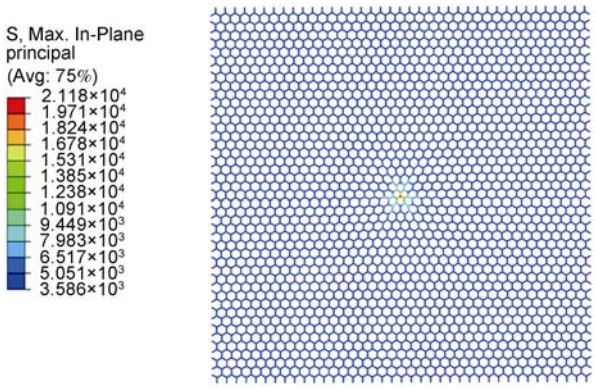

Figure 13 Stress distribution of a hexagon-mesh web, with the number of meshes 1778, the number of elements 5156, and the number of nodes 3554. The web's initial state is flat and slack. The boundaries are fixed tightly.

distributed. However, in the elements distant from these two cables, the stress decreases rapidly, which is a disadvantage for the strength of the whole web.

As Figure 13 illustrated, in the hexagon-mesh web, the maximum value of stress appears around the load point, and the stress decreases rapidly with the distance from the load point. In the elements with the same distance from the load point, the stress is almost equally distributed. That is, the hexagon-mesh web is capable of decentralizing the stress effectively and uniformly, so the strength of the hexagon-mesh web is supposed to be the highest among the three.

3.2.3 Equivalent strength

Commonly in the three webs, the maximum value of stress appears around the load point. Define equivalent strength and the max-stress, which approximately represents the capacity for the web to decentralize stress.

As illustrated in Figure 14, the equivalent strength of the hexagon-mesh web is the largest, followed by the square-mesh web, and the equivalent strength of the triangle-mesh web is the smallest among the three.

3.2.4 Equivalent stiffness

The vertical displacement of three webs represents the equivalent stiffness. Large vertical displacement corresponds to small stiffness as a whole web.

As illustrated in Figure 15, the equivalent stiffness of triangle-mesh web is the largest, followed by the square-mesh web, and the equivalent stiffness of the hexagon-mesh web is the smallest among the three.

3.3 Dynamic analysis

In the dynamical analysis, the capture process is highly nonlinear, because the deformation may be extremely large and the cable material property is also nonlinear.

In the capture process, the impact force changes sharply and rapidly, which was underscored by this part. When space webs are deployed, there may be no tensile force in the flexible webs for the microgravity in the orbit and the lack of support components. And since webs are too slack and flexible to resist any compressive force, there may be no formed configurations for them. While during the impact process, there is a sharp increase for internal force in the web and a large deformation in a short time.

Consider the triangle-, square- and hexagon-mesh webs provided with the same length of cable and the same total area. A rigid ball impacts the slack webs vertically with the same momentum. The dynamical response was simulated.

3.3.1 Impact deformation

Consider the triangle-mesh web with the number of meshes 1260, the number of elements 2014, the number of nodes 755, the square-mesh web with the number of meshes 1600, the number of elements 3120, the number of nodes 1677, and the hexagon-mesh web with the number of meshes

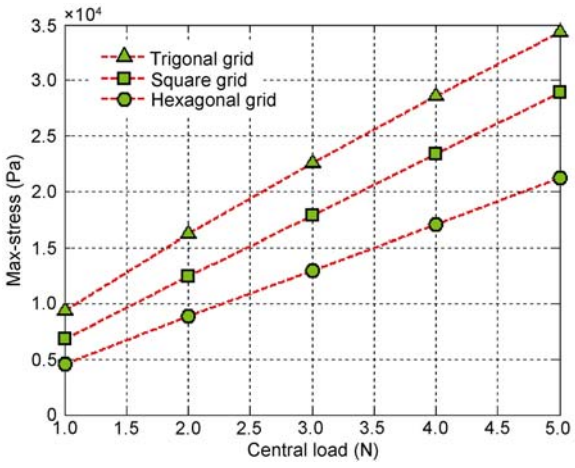

Figure 14 Max-stress in the webs under different loads, load 1, 2, 3, 4, 5 N concentrated pression on the centre point.

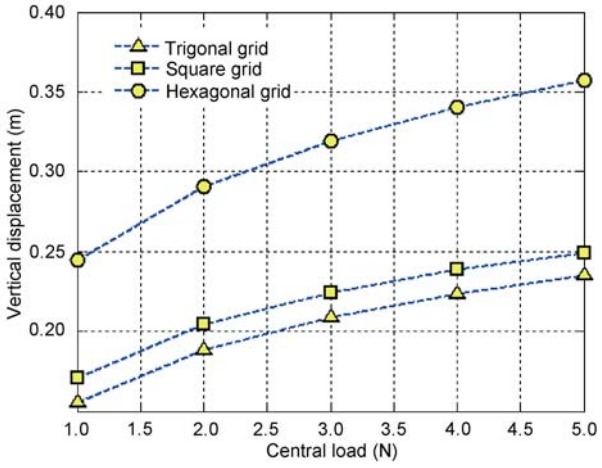

Figure 15 Vertical displacement of the webs under different loads, load 1, 2, 3, 4, 5 N concentrated pression on the centre point.

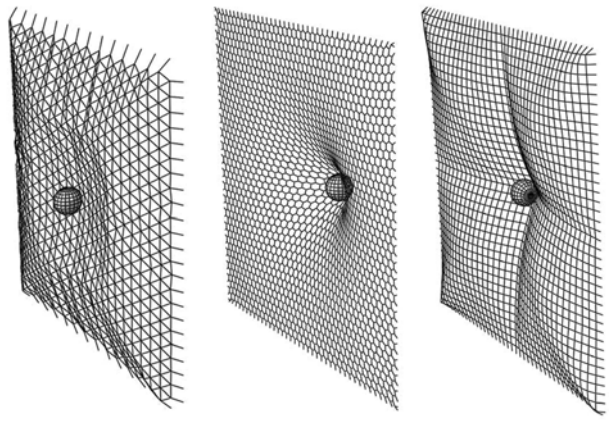

Figure 16 Impact deformation of the webs with different meshes. The vertical displacement of the contact point is different obviously.

1778, the number of elements 5156, and the number of nodes 3554. All the three webs are initially loose and slack while the boundaries are fixed tightly. Figure 16 illustrated the impact deformation of the three webs.

According to the simulation, harder oscillation is observed in the triangle-mesh web than that in the other two, showing more impact kinetic energy transferred to vibrational energy of the web.

3.3.2 Max-stress

The max-stress in the impact process represents the capacity of the webs to decentralize impact load.

As illustrated in Figure 17, small impact momentum leads to similar results to the static case. However, when the impact momentum increases, the max-stress in the square-mesh web becomes larger than that in the triangle-mesh web, since most elements in the square-mesh web lag behind the two cables crossing at the contact point, which responds rapidly at the crash moment, causing a sharp increased stress.

3.3.3 Global displacement

The vertical displacement of the webs in the impact process represents the buffering capacity of the webs.

As illustrated in Figure 18, similar to the static case, vertical displacement of the triangle-mesh web is the largest, followed by the square-mesh web, and the equivalent stiffness of the hexagon-mesh web is the smallest among the three.

4 Conclusions

This paper deals with the modelling of space webs and the static and dynamic behavior of webs with different meshes. To our knowledge, computational difficulties of flexible webs always exist due to several kinds of nonlinear factors, especially for the capture process, in which the nonlinearity caused by geometric, material, boundary condition and external load might coexist at the same time.

For the presented numerical method, truss element with the size equal to the mesh was adopted in the FE model in order to reduce the computational complexity. The cable material constitutive relationship was introduced into the model by an inline function. The parameterized modeling of webs with different types of meshes was implemented by a pre-processing program, and explicit time integration was employed to solve the governing equations of motion.

From the above, a parameterized modeling method with favorable generality for space webs was obtained. As an application, the static and dynamic response of webs with triangle, square and hexagon meshes was calculated under different conditions. The stress distribution and global deformation of the webs were discussed in statics, and special attention is paid to the max-stress and global deformation in the dynamic analysis.

In conclusion, the cable material property works well in the finite element model of space webs in statics and dynamics. Calculated results show that the cable material con-

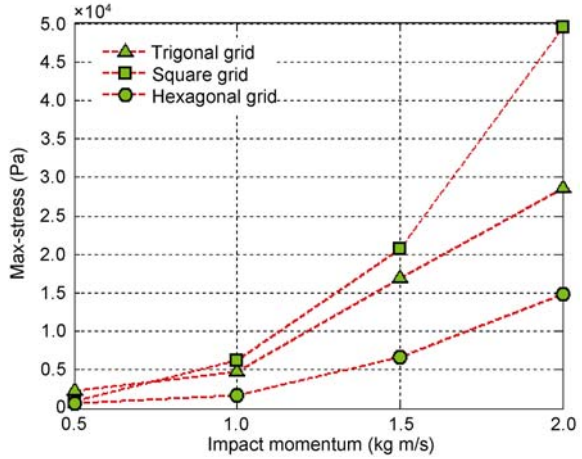

Figure 17 Max-stress of the webs under different impact momentums, with the value 0.5, 1.0, 1.5 and 2.0 kg m/s.

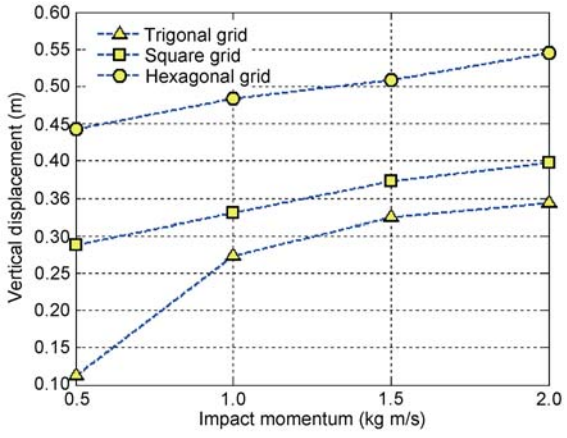

Figure 18 Vertical displacement of the webs under different impact momentums, with the value 0.5, 1.0, 1.5 and 2.0 kg m/s.

stitutive relationship provides better simulation of the behavior of slack flexible cable webs.

The following shows the analysis of webs with different types of meshes.

Hexagon-mesh web has low equivalent stiffness and high equivalent strength, that is, small element deformation and large global deformation, which may be a favourable buffering structure in capturing orbital objects. Besides, hexagon-mesh shape can effectively decrease the use of materials.

The square-mesh web has moderate equivalent stiffness and equivalent strength, while the stress in the web mainly concentrates on the two cables crossing at the contact point, which might be helpful to the capture prototype design.

The triangle-mesh web has high equivalent stiffness and low equivalent strength; therefore, its fundamental frequence is the highest among the three, which leads to a good damping characteristic.

1 Nakasuka S, Aoki T, Ikeda I, et al. "Furoshiki Satellite"—a large membrane structure as a novel space system. Acta Astronaut, 2001, 48: 461–468

2 Kaya N, Iwashita M, Nakasuka S, et al. Crawling robots on large web in rocket experiment on furoshiki deployment. J British Interplanet Soc, 2005, 58: 403–406

3 Kaya N. A new concept of SPS with a power generator/transmitter of a sandwich structure and a large solar collector. Space Energy Transp, 1996, 1: 205–213

4 Mankala K K, Agrawal S K. Dynamic modeling and simulation of impact in tether net/gripper systems. Multibody Syst Dyn, 2004, 11: 235–250

5 Palmerini G B, Sgubini S, Sabatini M. Space webs based on rotating tethered formations. Acta Astronaut, 2009, 65: 131–145

6 Gärdsback M, Tibert G. Deployment control of spinning space webs. J Guidance Control Dyn, 2009, 32: 40–50

7 Tibert G. Deployable Tensegrity Structures for Space Applications. Dissertation for the Doctoral Degree. Stockholm: Royal Institute of Technology Department of Mechanics, 2002

8 Mori O, Tsuda Y, Nishimura Y, et al. Deployment dynamics of clover type solar sail. In: 14th ISAS/JAXA Workshop on Astrodynamics and Flight Mechanics, Tokyo, Japan Aerospace GÄRDSBACK AND TIBERT 49 Exploration Agency Paper A-5, July 2004

9 Lader P F, Enerhaug B, Fredheim A, et al. Modelling of 3D net structures exposed to waves and current. In: Proceedings of the 3rd International Conference on Hydroelasticity in Marine Technology. Oxford, UK: Department of Engineering Science, The University of Oxford, 2003

10 Lader P F, Fredheim A, Enerhaug B, et al. Dynamic behaviour of 3D nets exposed to waves and current. In: Proceedings of the 20th International Conference on Offshore Mechanics and Arctic Engineering, Rio de Janeiro, Brazil, 2001

11 Priour D. Analysis of nets with hexagonal mesh using triangular elements. Int J Numer Meth Eng, 2003, 56: 1721–1733

12 Yu Y, Baoyin H X, Li J F. Modelling and simulation of space webs projecting dynamics. J Astronaut, 2010, 31: 1289–1296

13 Yu Y, Baoyin H X, Chen Y, et al. Static and dynamic analysis of space webs. In: 61st International Astronautical Congress, Prague, CZ, 2010

14 Zhu D P. The Large Deformation Curved Beam Element in Multibody Dynamics and Its Application. Dissertation for the Master Degree. Beijing: Tsinghua University, 2008

15 Shabana A A, Yakoub R Y. Three dimensional absolute nodal coordinate formulation for beam elements: Theory. ASME J Mech, 2001, 123: 606–613

16 Yakoub R Y, Shabana A A. Three dimensional absolute nodal coordinate formulation for beam elements: implementation and applications. ASME J Mech, 2001, 123: 614–621

17 Fujii F, Noguchi H, Osterrieder P. Static and dynamic large displacement response of flexible nets. In: International Symposium on New Perspectives for Shell and Spatial Structures, IASS-APCS 2003, Taipei, CD-ROM, 2003

18 Fujii F, Noguchi H. Flexible nets in statics and dynamics. In: European Congress on Computational Methods in Applied Sciences and Engineering, ECCOMAS 2004, Finland, 2004